

# Optics Diffraction and the FPE

Charles L. Rino

<http://chuckrino.com/wordpress/>

May 31, 2011

## Abstract

This paper explores the equivalence between spherical wave and plane propagators. Spherical wave propagators are intrinsically part of diffraction and boundary scattering theory. However, one can construct mathematically equivalent representations of propagating waves from plane-wave superpositions. In effect, this leads to two distinctly different approaches to diffraction theory. As a practical matter, common computational methods apply when wavelength does not drive sampling requirements, which is largely confined to Fraunhofer diffraction. Fresnel scattering can lead to wavelength driven sampling, which severely limits computational methods. Examples are presented to illustrate the Fourier-domain methods.

## 1 Introduction

Radio frequency (RF) and optical remote sensing applications employ diverse technologies, but they have common theoretical foundations. The essential physics is captured by the time-harmonic form of the Helmholtz equation:

$$\nabla^2 \psi(\mathbf{r}) + k^2(\mathbf{r}) \psi(\mathbf{r}) = 0. \quad (1)$$

The spatially varying complex wavefield,  $\psi(\mathbf{r})$ , is the observable, and  $k(\mathbf{r})$  is formally the magnitude of a local propagation vector. The diverse technologies are driven by the substantial difference in operating wavelengths. Nonetheless, there is a broad class of propagation problems where wavelength does not dictate sampling requirements. In this operating regime identical computational methods can be used. This observation is not novel, but it provides an interesting framework for interpreting propagation theory.

Coincidentally, this commonality was captured in a recent development of the theory of scintillation as an extension of propagation theory that accommodates *weakly inhomogeneous media*. [1] Strictly homogeneous structure (constant  $k^2$ ) is replaced by structure with gradients constrained to be small over wavelength scales. Backscatter can be neglected insofar as its effects on the forward propagation from directed sources are concerned. The resulting

forward-propagation phenomena are fully characterized by a single first-order differential equation called the forward propagation equation (FPE). The more familiar parabolic wave equation (PWE) can be derived from the FPE. Ray optics, in turn, can be derived from the PWE.

PWE applications are well-established for applications involving optics and RF as well as acoustics. As an example, consider the intensity of an optical field measured with a focal-plane array of detectors. The intensity at each detector can be characterized by the ray-path from a source point through the focal distance from the center of the array to the focal plane location. Propagation disturbances initiated by atmospheric refractive-index structure along the ray path are readily accommodated by the PWE. An antenna tracking an RF source senses ionospheric propagation disturbances along the ray path from the source to the receiver in much the same way. Although the physical scales of the applications and the physics that drive the constitutive relations differ, the propagation model and the sampling requirements are nearly identical.

The FPE uses a Fourier-domain (plane-wave) propagator, which solves (1) exactly in the absence of structure. Optics-oriented treatments of the propagation phenomena invariably start with the Huygens-Fresnel (spherical-wave) construction, which also solves (1) exactly in the absence of structure. The exact solution here referred to here is the free propagation of the source field. Because both the plane-wave and spherical-wave total field representations satisfy the Helmholtz equation, there is an implied equivalence between the two approaches. The theory of diffraction characterizes interference phenomena that develop as EM waves propagate away from their source regions. The aforementioned equivalence implies that the theory of diffraction itself can be formulated with plane-wave or spherical-wave propagators.

An important distinction is made here between the theory of scattering, which formally addresses the interaction of EM waves with material objects bounded by surfaces, and the interference phenomena (diffraction) that results. Unfortunately, solutions to the Helmholtz equation that accommodate embedded surfaces and compact objects are not easily obtained. Indeed, the boundary-integral formulation of EM scattering theory admits no analytic solutions whatsoever.<sup>1</sup> Moreover, numerical solutions to the boundary-integral equations that define the source fields require sub-wavelength sampling. Wavelength scale sampling severely limits practical analytic exploration. Consequently, most practical applications of scattering theory use approximate boundary conditions.

To pursue the ramifications, recall that Green's theorem facilitates the construction of solutions to the Helmholtz equation as superpositions of the radiation from induced sources on the boundary surfaces. Kong's development of EM boundary scattering theory, for example, is presented as the mathematical formulation of Huygen's principle. [2, Chapter 5.3] Physical optics is derived from the scalar form of Green's theorem, which is a special case of that mathe-

---

<sup>1</sup>The known boundary-constrained analytic solutions to the Helmholtz equation use special coordinate systems that support complete sets of basis functions that match boundary conditions intrinsically.

mathematical formulation. The guiding construct is the generation of secondary EM fields initiated on boundaries and propagated as a superpositions of spherical waves. That part of the problem is robust.

If, as is usually the case, the boundary surfaces can be isolated by parallel planes, then, via the aforementioned equivalence, propagation away from the isolating planes can be calculated exactly by using Fourier decompositions rather than as extensions of the evolving spherical waves. Because the fields near singular sources are highly structured, it is often more efficient to use plane-wave decompositions. This is the effectively the formal basis for constructing wave-wave scattering cross sections, Fourier optics, and the FPE and the PWE methodology already introduced.

It is appropriate to note as well that the common manifestations of diffraction, such as the finite width of the point-spread-function in the focal plane of a lens system and the penetration of fields into geometric shadow regions are interference patterns that develop as waves propagate away from their sources. The development of intensity scintillation is also a manifestation of diffraction. Indeed, under some conditions strong-focusing produces dramatic fine-grained intensity patterns called *diffractals* [3].<sup>2</sup> To reiterate, although diffraction phenomena are intimately related to starting fields, the interference patterns evolve through propagation.

This paper reviews the mathematical equivalence between plane-wave and spherical propagation, with emphasis on well-known results usually presented as part of diffraction theory, specifically Fraunhofer and Fresnel diffraction and the well-known Fourier-transform relation between a focusing lens aperture stop and the point-spread function in the focal plane. Examples show that mathematical equivalence does not imply equivalent computational demands. A rigorous test of the formal plane-wave spherical-wave propagator equivalence is the computation of the field from the aperture stop of a focusing system through the focal point. As a practical matter, only the Huygens-Fresnel construction supports this calculation at optical wavelengths precisely because it demands near wavelength-scale sampling.

## 2 Background

The starting point for the theoretical development is the scalar Helmholtz equation. In a medium that admits refractive index variations, the Helmholtz equation is written in the following modified form, which explicitly identifies the structure variation [1, Chapter 2]:

$$\nabla^2 \psi + k^2 \psi = -k^2 (2\overline{\delta n} + \overline{\delta n}^2) \psi. \quad (2)$$

As noted in the introduction,  $\psi(\mathbf{r})$  is the observable time-harmonic complex field. It is convenient to identify a constant mean reference background refrac-

---

<sup>2</sup>See also the cover of the July 1984 issue of *Applied Optics*.

tive index  $\bar{n}$  such that  $\overline{\delta n} = \delta n/\bar{n}$ . It follows that

$$n = \bar{n} (1 + \overline{\delta n}). \quad (3)$$

The background refractive index is absorbed in the wavenumber definition

$$k = 2\pi f\bar{n}/c = 2\pi/\bar{\lambda}, \quad (4)$$

where  $f$  is the temporal frequency. For most scintillation applications the perturbations are small enough that the quadratic term can be ignored; moreover, the remaining occurrences of  $\bar{n}$  can be replaced by unity. For example, the refractive index of the atmosphere is usually reported in refractivity units defined as  $(n - 1)10^6$ . However, optical glass may have a refractive index of 2 or more, which emphasizes the extreme differences of the propagation phenomena.

Equation (2.2) in Rino [1] is the vector form of (2). Equation (3-8) in Goodman[4] is the time-domain form of the parent equation that leads to (2). The derivation of the underlying modified form of the Helmholtz equation neglects the term,  $\nabla(\mathbf{E} \cdot \nabla \ln n)$ . In Rino [1] *weakly inhomogeneous media* makes this approximation explicit. As it is applied for analysis, Equation (3-13) in Goodman [4] is equivalent to (2). The time variation of the complex fields,  $\exp\{-2\pi i f t\}$ , is implicit.

## 2.1 Boundary Integral Representations

As noted in the introduction, boundary integral representations are used to characterize the interaction of EM waves with material objects and boundary surfaces. The development in Goodman[4] follows Born and Wolf [5], which starts with the scalar boundary-integral representation

$$\psi(\mathbf{r}) = \iint_{\Sigma} \left[ \frac{\partial \psi(\mathbf{r}_s)}{\partial N} G(\mathbf{r}, \mathbf{r}_s) + \psi(\mathbf{r}_s) \frac{\partial G(\mathbf{r}, \mathbf{r}_s)}{\partial N} \right] ds. \quad (5)$$

In (5),  $\psi(\mathbf{r})$  represents the complex field in the unbounded region outside the boundary  $\Sigma$ , and

$$G(\mathbf{r}, \mathbf{r}_s) = \frac{\exp\{ik|\mathbf{r} - \mathbf{r}_s|\}}{|\mathbf{r} - \mathbf{r}_s|}, \quad (6)$$

is the scalar Green function. One can show that  $\psi(\mathbf{r})$  is a formal solution to Helmholtz equation by virtue of the singular behavior of the Green function as  $\mathbf{r} \rightarrow \mathbf{r}_s$ . The Green function and its normal derivative propagate induced fields on the boundary surfaces throughout the exterior region. A radiation condition eliminates contributions from the outer boundary that closes the Green theorem surface.

A self-consistent determination of the induced boundary fields requires knowledge of the electric properties of the medium inside the boundary as well as the boundary surface geometry. For impenetrable surfaces, the boundary integral can be manipulated as written to determine the induced fields. Equations that can be solved for the unknown source fields can be obtained by taking

the limit as  $\mathbf{r} \rightarrow \mathbf{r}_s$ , but in doing so one must accommodate the singular behavior of the Green function and its normal derivative. However this is done, stable results demand sub-wavelength sampling.

Most practical applications of boundary-integral representations approximate the induced fields with scaled representations of the source fields. By comparison, in the derivation of the FPE the multiplicative interaction of the total field with the material structure permits an exact evaluation of the integral representation. Converting the integral equation into a pair equivalent differential equations isolates the propagation interaction and the media interaction terms. In a homogeneous medium it can be established directly that the propagation operator satisfies the homogeneous Helmholtz equation exactly.

For reference, the essential elements of theory of diffraction as it is developed for optical systems are captured by the Dirichlet integral representation

$$\psi(\mathbf{r}) = \iint_{\Sigma} U(\mathbf{r}_s) G(\mathbf{r}, \mathbf{r}_s) ds, \quad (7)$$

where  $U(\mathbf{r}_s)$  is a source function on a representative surface. If  $U(\mathbf{r}_s)$  represents an evolving spherical wavefront, (7) is a mathematical statement of the Huygens-Fresnel construction. The equivalence that will be established later is readily generalized to forms of the theory that incorporate the derivative (Neumann) term and extensions vector fields, but the additional algebraic complexity can obscure the essential characteristics of the result.

## 2.2 The Forward Approximation

The theoretical development in [1, Chapter 2] avoids an explicit treatment of scattering theory by exploiting the fact that propagating waves, however they are initiated, are highly directed. This is made explicit by showing that (2) admits an equivalent representation as a pair of coupled first-order differential equations. The coupled equations individually characterize wave fields that propagate in opposite directions with respect to a prescribed reference axis. In the absence of the weakly inhomogeneous structure that couples the equations, the solutions are uncoupled and exact. A unidirectional source excites waves propagating in the opposite direction only through scattering interactions within the medium. These scattering interactions are negligibly small in a weakly inhomogeneous medium. The forward approximation neglects the weak backscatter insofar as it affects the forward field are concerned.

The result is a single first-order differential equation, which is called the forward propagation equation (FPE). The following scalar FPE fully characterizes propagation in an unbounded weakly inhomogeneous medium:

$$\frac{\partial \psi(x, \varsigma)}{\partial x} = \Theta \psi(x, \varsigma) + ikS(x, \varsigma; \lambda) \psi(x, \varsigma). \quad (8)$$

In (8)  $\psi(x, \varsigma)$  represents the complex wave field in a rectangular coordinate system with  $x$  the propagation reference axis and  $\varsigma$  a position vector in the

plane normal to the  $x$  direction, and  $k = 2\pi/\lambda$  is the wave number. The source function is derived from the departure of the refractive index from unity:

$$(n^2 - 1)/2 = \delta n + \delta n^2/2, \quad (9)$$

and

$$\begin{aligned} S(x, \varsigma; \lambda) &= \delta n(x, \varsigma; \lambda) + \delta n(x, \varsigma; \lambda)^2/2 \\ &\simeq \delta n(x, \varsigma; \lambda). \end{aligned} \quad (10)$$

The leading term in (8) represents the propagation of a coherent monochromatic wave field in a homogeneous medium. The exact form of the propagation operator is

$$\begin{aligned} \Theta\psi(x, \varsigma) &= \iint \widehat{\psi}(x_0, \kappa) \exp\{\pm i k g(\kappa)(x - x_0)\} \\ &\quad \times \exp\{i\kappa \cdot \varsigma\} \frac{d\kappa}{(2\pi)^2}. \end{aligned} \quad (11)$$

The complex field,  $\widehat{\psi}(x_0, \kappa)$ , is the two-dimensional Fourier transform of the field in the plane at  $x = x_0$

$$\widehat{\psi}(x_0, \kappa) = \iint \psi(x_0, \varsigma) \exp\{-i\kappa \cdot \varsigma\} d\varsigma, \quad (12)$$

and

$$g(\kappa) = \begin{cases} \sqrt{1 - (\kappa/k)^2} & \text{for } \kappa \leq k \\ i\sqrt{(\kappa/k)^2 - 1} & \text{for } \kappa > k \end{cases}. \quad (13)$$

Irrespective of how the FPE was derived, one can readily verify by direct substitution that (11) satisfies (2) when  $\delta n = 0$ . Thus, solutions to the FPE in a homogeneous medium are exact solutions to the homogeneous Helmholtz equation. The unnumbered equation in Section 3.10.4 of Goodman [4] is equivalent to (11),<sup>3</sup> but Goodman does not use it in subsequent developments.

### 2.2.1 Narrow-angle scatter

For numerical integration of the FPE, the narrow-angle approximation is neither required nor advantageous. However, the narrow-angle scatter approximation is essential for analytic computation. When the spectral content of the field  $\widehat{\psi}(x_0, \kappa)$  is well contained within the disk defined by  $\kappa = k$ , one can use the approximation

$$g(\kappa) \cong 1 - (\kappa/k)^2/2. \quad (14)$$

---

<sup>3</sup>In Rino [1] the propagator is defined in terms of spatial frequencies represented by  $\kappa = [\kappa_y, \kappa_z]$  where  $\kappa_y = 2\pi/L$  rather than spatial frequencies.

The Formal equivalence of multiplication in the Fourier domain by powers of  $\kappa$  and derivatives of the same order in the spatial domain leads to the following formal definition of the diffraction-operator and the parabolic approximation:

$$\begin{aligned} ik\Theta &= ik\sqrt{1 + \nabla_{\perp}/k^2} \\ &\cong ik + i\nabla_{\perp}/(2k). \end{aligned} \quad (15)$$

The parabolic approximation (8), namely

$$\frac{\partial U(x, \varsigma)}{\partial x} = i\nabla_{\perp}U(x, \varsigma)/2k + ik\delta n(x, \varsigma)U(x, \varsigma), \quad (16)$$

is obtained by applying (15) and performing some straightforward manipulations. The PWE solutions apply to the modified field

$$U(x, \varsigma) = \psi(x, \varsigma) \exp\{-ikx\}, \quad (17)$$

however; removal of  $\exp\{-ikx\}$  in the FPE does not influence computational requirements.

### 2.3 Ray Optics

The theory of ray optics is derived by approximating vector fields by products of the form  $\mathbf{A}(x, \varsigma) \exp\{ik\phi(x, \varsigma)\}$ . The refractive index is treated as a continuous variable. When the refractive index gradients are small, which is a necessary condition for weakly inhomogeneous media, the evolving field structure can be characterized by propagation along geometric ray paths. The ray trajectories are defined by position-dependent vectors  $\mathbf{r}(s)$ , where  $s$  is the distance along the ray. The vector  $\mathbf{r}(s)$  is constrained locally by two orthogonal vectors, namely the unit vector  $\mathbf{s}$  tangent to the ray at  $\mathbf{r}(s)$  and the curvature vector  $\varkappa = ds/ds$ , which is normal to  $\mathbf{s}$ . The ray trajectory in the medium must satisfy the ray equation

$$n\varkappa + \frac{dn}{ds}\mathbf{s} = \nabla n. \quad (18)$$

This equation can be derived from (16) by assigning the phase variation  $\exp\{ik\phi(x, \varsigma)\}$  to  $U(x, \varsigma)$ [6, Chapter 5.2]. This is the basis for the earlier claim that ray optics in unbounded media is contained in the broader class solutions to the FPE. Note that aside from the wavelength dependence of the refractive index, the ray trajectories are wavelength independent.

### 2.4 Optical Lens Systems

Optical lens systems require special treatment for two reasons. First, a lens is defined by discontinuous boundaries, which often have discontinuous normal derivatives as well. Second, the diffraction effects that limit the resolution of optical systems ultimately must be incorporated into the analyses. A highly simplified lens system is used here to illustrate the use of ray optics to approximate a starting field for Fourier-domain computation.

Consider a representative lens system constructed from a colinear arrangement of homogeneous radially symmetric lens objects. For simplicity, lens objects will be confined to closed volumes circumscribed by intersecting spherical segments. As already noted, boundary scattering theory tells us that the transmission and scattering (reflecting) properties of lens objects are determined by the shape of the defining boundary surfaces and the constitutive properties of the lens material. The dielectric properties are defined by a frequency-dependent refractive index. From ray theory it follows that ray paths within homogeneous lens objects are straight lines.<sup>4</sup>

A planar boundary admits an exact solution that can be constructed by applying Snell's law to determine the wavefront propagation directions on either side of the boundary:

$$\frac{\sin \theta_1}{\sin \theta_2} = \frac{n_2}{n_1}. \quad (19)$$

If the boundary variations are smooth enough, the boundary conditions are approximated by applying Snell's law with respect to the surface normal. The implicit assumption here is that the lens system is sufficiently uniform that rays can be approximated by straight lines inside lens objects. Thus, ray segments can be defined by unit vectors,  $\mathbf{u}_i$ , where  $i$  corresponds to the side of the boundary in which the ray is defined. Let  $\mathbf{u}_n$  represent a unit vector normal to the surface. At the boundary

$$\mathbf{u}_i \cdot \mathbf{u}_n = \cos \theta_1,$$

which defines  $\sin \theta_1$ . Snell's law defines  $\sin \theta_2$ , which is measured with respect to  $-\mathbf{u}_n$ . The following pair of equations define the continuation of ray trajectories within lens objects:

$$-\mathbf{u}_n \cdot \mathbf{u}_2 = \sqrt{1 - \sin^2 \theta_2} \quad (20)$$

$$-\mathbf{u}_n \times \mathbf{u}_2 = \sin \theta_2 \quad (21)$$

Knowing  $\mathbf{u}_2$ , one can calculate the intersection of the ray with the opposite lens cap. The process can then be repeated to determine the direction of the rays exiting the lens object. There are many utilities available that will perform completely general ray analyses of lens systems and report the results graphically or in tabular form. However, the simpler formulation is useful for illustrative purposes. Figure 1 shows the evolution of a bundle of paraxial rays through a bispherical lens. The cap radii are 120 mm. The lens thickness is 10 mm. The refractive index at  $.46 \mu$  is 1.62. The red pentagram show the nominal location of the focus calculated from the lens equation

$$\frac{1}{f} = (n - 1) \left( \frac{1}{r_1} - \frac{1}{r_2} + \frac{(n - 1)}{n} \frac{d}{r_1 r_2} \right), \quad (22)$$

where  $\pm r_n$  is the positive convex radius of curvature of the lens faces, and  $d$  is the thickness of the lens along the central ray.

<sup>4</sup>For this development only monochromatic radiation will be considered.

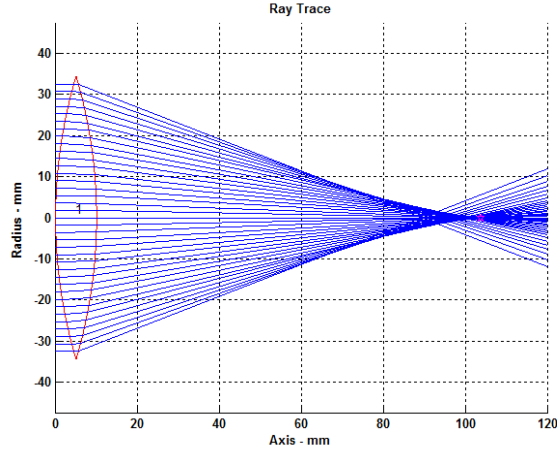


Figure 1: Vertical cross section of the ray-trace evolution of a parallel bundle of rays interacting with a bispherical lens. The red pentagram shows the predicted focal point.

#### 2.4.1 Field Estimation

The ray-optics construction of the wavefield propagating away from the lens system can be used to estimate the field in the aperture plane. Consider the normal plane at  $x = 10$  mm. The optical path is defined as the ray-path integral weighted by the refractive index:

$$s = \oint n ds = \sum_i n_i s_i. \quad (23)$$

The summation is over the three straight-line paths that connect points in the entrance plane to points in the exit plane. The complex field in the vertical plane has the form

$$\psi(x, \zeta') = A(x, \zeta') \exp\{iks(\zeta')\}. \quad (24)$$

The amplitude weighting accounts for the increased field intensity necessary to conserve energy as the field intensity becomes more concentrated. Figure 2 shows the optical path computed at the exit plane of the lens object shown in Figure 1.

An eighth-order polynomial fit was used to approximate the optical path for subsequent analysis.

Figure (3) shows the difference between a purely quadratic phase variation and the phase variation deduced from ray-optics for the bispherical lens. It can be seen that the departures become more pronounced as the edges of the lens are approached. In effect the full resolving power of the lens as dictated by its diameter cannot be realized.

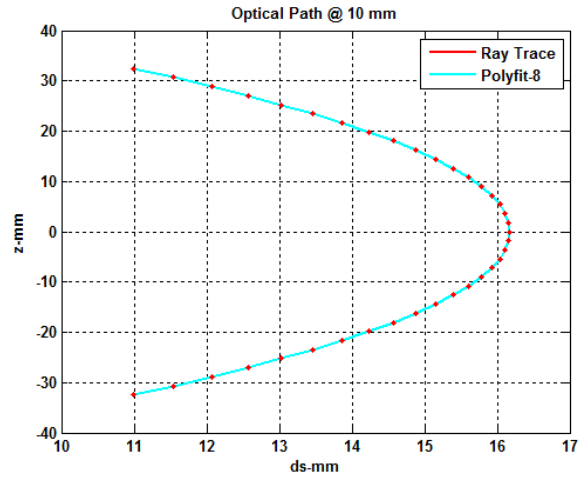


Figure 2: Optical path length (red dots) computed from ray-trace shown in Figure 1. Cyan curve is fit to 8th order polynomial.

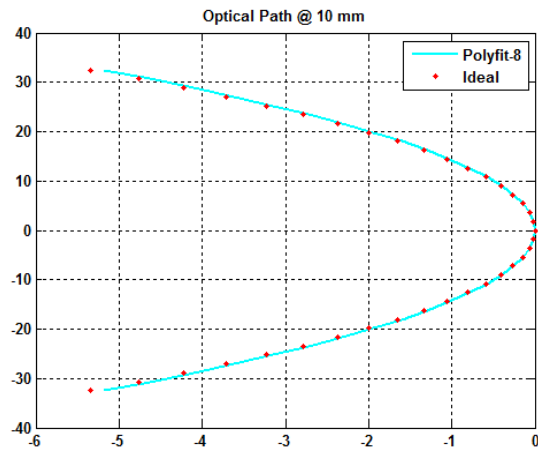


Figure 3: Ideal phase correction to produce a focus at a distance  $f$  from the aperture plane.

## 2.5 Forward Propagation

This section derives the Fraunhofer and Fresnel approximations from the FPE propagator and demonstrates the formal equivalence between the Huygens-Fresnel integral representation and the FPE. The standard approximations use the narrow-angle scatter approximation, but the Fourier-domain propagator can be applied in principle without constraint. The examples show that wavefront curvature imposes severe computational requirements. Although Huygens-Fresnel requires the same sample density, it allows localization of the computation. For this reason Huygens-Fresnel is the only viable construct for calculating diffraction effects at optical wavelengths for high-curvature wavefields.

Because narrow-angle scatter is the norm for practical optical systems, the Fourier transform relation between uniform aperture and the point-spread-function in the focal plane can be used modest sampling requirements.

### 2.5.1 Full-Wave Diffraction

In an unobstructed homogeneous region, the solution to the scalar Helmholtz equation is determined by the field in the aperture plane at  $x = x_0$ . If the aperture plane is tilted, a linear phase variation can be applied to launch the wavefield normal to the actual orientation of the plane[7]. Alternatively, the propagator itself can be written for evaluation along the principal propagation direction[1, Chapter 4]. However, for the purposes of the development here these details are unimportant. Basically (11) is a general solution to (1) for any field defined in an unobstructed plane.

If one is interested in the field only at a large distance from the plane, the solution takes a particularly simple form. An application of the stationary phase approximation to (11) will show that

$$\lim_{\Delta x \rightarrow \infty} \Theta \psi(\Delta x, \varsigma) = -ig(\kappa_r) \left[ k^2 \widehat{\psi}(0; \kappa_r) \right] \frac{\exp\{ikr\}}{2\pi kr}, \quad (25)$$

where  $r = \sqrt{\Delta x + \varsigma^2}$  and  $\kappa_r$  is the transverse wavenumber in the direction of  $\mathbf{r} = [\Delta x, \varsigma]$ . It is fundamental to the design of remote sensing systems because it defines the on-axis signal intensity at distance  $r$  from the source. Off axis, the field variation is defined by the Fourier transform of the aperture distribution. In optics literature, (25) is called Fraunhofer approximation [4, Chapter 4]. Although the narrow-angle scatter approximation was not used in derivation, narrow-angle scattering is implicit because the transverse dimensions are necessarily small when  $\Delta x \rightarrow \infty$ .

The near-field is much more demanding. To explore the near field, it is

convenient to rewrite (11) as an explicit linear operation on the starting field:

$$\begin{aligned} \Theta\psi(x, \varsigma) &= \iint \left[ \iint \psi(x_0, \gamma/k) \exp\{-i\eta \cdot \gamma\} d\gamma \right] \\ &\quad \times \exp\left\{i\sqrt{1-\eta^2}(k\Delta x)\right\} \exp\{i\eta \cdot k\varsigma\} \frac{d\eta}{(2\pi)^2}. \end{aligned} \quad (26)$$

Changing the order of integration isolates a nominally singular inner integral:

$$\begin{aligned} \Theta\psi(x, \varsigma) &\approx \iint \psi(x_0, \gamma/k) \\ &\quad \times \left[ \iint \exp\left\{i\sqrt{1-\eta^2}(k\Delta x)\right\} \exp\{i\eta \cdot ((k\varsigma) - \gamma)\} \frac{d\eta}{(2\pi)^2} \right] d\gamma, \end{aligned} \quad (27)$$

However, the exchange is justified when the spectral content of the starting field is limited to a narrow range of propagation angles, say where  $\sqrt{1-\eta^2} \simeq 1 - \eta^2/2$ . It then follows that

$$\begin{aligned} \Theta\psi(x, \varsigma) &\simeq \exp\{ik\Delta x\} \iint \psi(x_0, \gamma/k) \\ &\quad \times \iint \exp\{-i\eta^2(k\Delta x/2)\} \exp\{i\eta \cdot ((k\varsigma) - \gamma)\} \frac{d\eta}{(2\pi)^2} d\gamma. \end{aligned} \quad (28)$$

The Fourier transform represented by the  $\eta$  integration can be evaluated analytically. Carrying out the integration leads to the following near-field form of the equation, which is called the Fresnel approximation

$$\begin{aligned} \Theta\psi(\Delta x, \varsigma) &\simeq \frac{-ik \exp\{ik\Delta x\}}{2\Delta x} \\ &\quad \times \iint \psi(0, \varsigma'') \exp\left\{i(\varsigma - \varsigma'')^2 k / (2\Delta x)\right\} d\varsigma'' \quad (29) \\ &= \frac{-ik \exp\{ik\Delta x\}}{2\Delta x} \exp\{i\varsigma^2 k / (2\Delta x)\} \\ &\quad \times \iint [\psi(0, \varsigma'') \exp\{i\varsigma''^2 k / (2\Delta x)\}] \exp\{-i\varsigma \cdot \varsigma'' (k/\Delta x)\} d\varsigma'', \end{aligned} \quad (30)$$

The two forms of the result are identical to Goodman's Equations (4-14) and (4-17). The fact that the final form of the Fresnel approximation is itself a Fourier transformation should not be confused with the Fourier transformation in the propagation integral (26), which involves no approximations.

The reason for deriving these well known results here is to show that they are special cases of full wave propagation, which can be evaluated numerically by using Fourier transformations. Moreover, there is no compelling reason to

impose the narrow scatter approximation. For the Fraunhofer regime, this is empty generality because there are few, if any, practical situations where the narrow-angle scatter approximation is violated. This is manifestly not the case in the Fresnel region. To explore this, consider the Huygens-Fresnel construction, which is also exact insofar as the propagation of a known starting field is concerned. The main difference is that the Huygens-Fresnel starting field is defined on a surface that need not be planar.

Starting with Huygens-Fresnel, consider the field in a plane at  $x = x_0$  that isolates the defining surface from an unobstructed propagation space. From (7),

$$\psi_{HF}(x_0, \varsigma) = \iint_{\Sigma} U(\mathbf{r}_s) \frac{\exp\{ik|x_0 - x_s, \varsigma - \varsigma_s|\}}{|x_0 - x_s, \varsigma - \varsigma_s|} ds. \quad (31)$$

Substituting the Weil representation of the Green function,

$$\frac{\exp\{ik|\Delta x, \varsigma - \varsigma'|\}}{|\Delta x, \varsigma - \varsigma'|\}} = \iint \frac{i \exp\{ikg(\kappa)\Delta x\}}{2kg(\kappa)} \exp\{i\kappa \cdot (\varsigma - \varsigma')\} \frac{d\kappa}{(2\pi)^2}, \quad (32)$$

into (31) and reversing the order of integration as before shows that

$$\begin{aligned} \psi_{HF}(x, \varsigma) &= \iint_{\Sigma} U(\mathbf{r}_s) \iint \frac{i \exp\{ikg(\kappa)\Delta x\}}{2kg(\kappa)} \exp\{i\kappa \cdot (\varsigma - \varsigma_s)\} \frac{d\kappa}{(2\pi)^2} ds \\ &= \iint \left[ \frac{i}{2kg(\kappa)} \iint_{\Sigma} U(\mathbf{r}_s) \exp\{-i\kappa \cdot \varsigma_s\} ds \right] \exp\{i\kappa \cdot \varsigma\} \\ &\quad \times \exp\{ikg(\kappa)\Delta x\} \frac{d\kappa}{(2\pi)^2}. \end{aligned} \quad (33)$$

Evaluating the two-dimensional Fourier transform of  $\psi_{HF}(x_0, \varsigma)$ <sup>5</sup> establishes the equivalence

$$\widehat{\psi}_{HF}(x_0, \kappa) = \frac{i}{2kg(\kappa)} \iint_{\Sigma} U(\mathbf{r}_s) \exp\{-i\kappa \cdot \varsigma_s\} ds. \quad (34)$$

Rewriting (33) in terms of  $\widehat{\psi}_{HF}(x_0, \kappa)$  reproduces the plane-wave propagator:

$$\psi_{HF}(x, \varsigma) = \iint \widehat{\psi}_{HF}(x_0, \kappa) \exp\{ikg(\kappa)\Delta x\} \frac{d\kappa}{(2\pi)^2}. \quad (35)$$

Note that (34) defines the Fourier transformation as an integration over the induced sources of the field. It shows as well the subsequent propagation of that field can be calculated in principle without approximation using Fourier-domain methods.

However, the factor  $1/g(\kappa)$  in (34) is singular at  $k = \kappa$ . For  $k < \kappa$  it has little effect; moreover, to properly accommodate the singularity requires careful

<sup>5</sup> $\Delta x = 0 \Leftarrow x = x_0$

evaluation. The poles in the spatial Fourier domain are necessary for generating the singular behavior of the Green function. With the singular points in the source region well removed from the plane at  $x = x_0$ , this term can be safely ignored.

Reciprocity provides another example of the equivalence between Green-function and plane-wave representations. The Green function is intrinsically symmetric to an interchange of the source and field point variables, which leads to the reciprocal interchange between a source point and a measurement point. It is also true that a spectral domain representation that maps incident plane waves to forward or scattered plane waves can be constructed for invariance to an interchange of wave vectors. [8].

### 3 Numerical Examples

The background material introduced two integral representations of a propagator that can be used for computing the evolution of a starting field. To the extent that the computation is to be done numerically, sampling requirements dictate the complexity. Strictly speaking, the Fourier domain propagator is not restricted by narrow-angle scattering constraints. However, most practical applications involve the Fraunhofer regime. If the split-step Fourier-domain method is used to solve the FPE, there is no practical reason to approximate the propagation operator. However, spatial-domain implementation of the diffraction operator is a finite difference method that does have advantages for propagation over very large distances in varying media.

The Fresnel region is much more challenging, although the practical problems that require near-field treatment are largely confined to focusing systems. In principle Fourier-Domain methods can be used, but the sampling requirements are defined by wavelength. An exception is computation of the field near the Focal plane of an imaging system, which violates narrow-angle scatter, but still satisfies a stationary phase condition that makes the Fourier-transform relation work. The following numerical examples of Fraunhofer and Fresnel diffraction illustrate the generality and limitations of Fourier-domain methods.

#### 3.0.2 Fraunhofer Diffraction

The first example uses a zero-phase starting field defined in a plane. A uniform circular “top hat” is a convenient realization because it admits an exact

transform:

$$\begin{aligned}
\widehat{\psi}(x_0, \kappa) &= \iint_{-D/2}^{D/2} \exp\{-i\zeta \cdot \kappa\} d\zeta \\
&= \int_0^D \int_0^{2\pi} \exp\{-i\kappa\zeta \cos\phi\} d\phi d\zeta \\
&= \frac{2\pi}{\kappa^2} \int_0^{\kappa D} \eta J_0(\eta) d\eta = \frac{2\pi D}{\kappa} J_1(\kappa D). \tag{36}
\end{aligned}$$

From (30), the field in the focal plane of a lens is

$$\psi(f, \varsigma) \sim \frac{2\pi f D}{k\varsigma} J_1(k\varsigma D/f).$$

The standard estimate of the focal spot size

$$d = 1.22\lambda f/D, \tag{37}$$

follows [4, Equation (4-32)].

Consider a uniform circular  $0.46 \mu$  source with diameter  $D = 68.56$  mm, which is the maximum extent of the lens used in the ray-trace example. Standard discrete Fourier transform (DFT) sampling requirements establish the relation

$$\Delta L \Delta K = \frac{2\pi}{N}.$$

Since the power-spectrum of the complex wavefield is invariant to propagation, the source field determines the sampling interval. In the far-field the beam will expand at a rate dictated by the angular extent of the Fourier-transform of the disc normalized to wavenumber. Since the expanding beam must stay within the computation grid to minimize edge effects, a span of  $5D$  was used to accommodate a propagation distance of  $10 m$ . Note that although  $D/\lambda = 1.5 \times 10^5$ , adequate sampling was achieved on a  $4096 \times 4096$  grid with  $\lambda/dy = \lambda/dz = 364$ .

Figure 4 shows a the vertical plane intensity for 50 logarithmically spaced propagation steps. The field has been normalized to its on-axis peak, which should be constant when the Fraunhofer limit is achieved. Logarithmic propagation steps were used to capture the evolution from the near field to the far-field limiting form. One can verify that the sidelobes are predicted by the Fourier transform of the disk. It is interesting that in the point-spread function in the focal plane of a lens (30) has the same shape.

Each computation step requires forward and inverse DFTs with in intervening matrix multiplication. The computation used approximately 20 s per step on a 64-bit, dual-processor PC with 8 GBytes of memory.

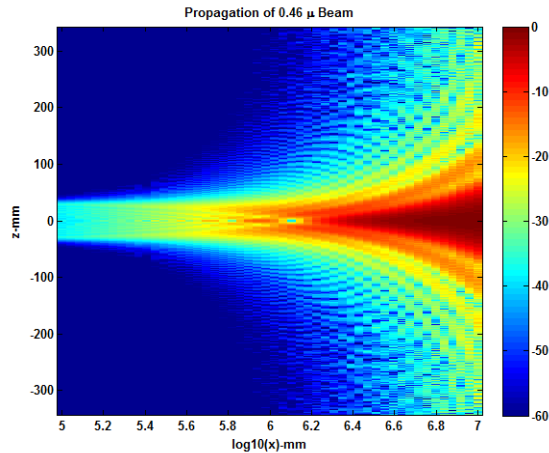


Figure 4: FPE computation of the forward propagation of an unfocused circular spot. The field intensity is a vertical slice of the two-dimensional field multiplied by the square of the propagation distance.

If one were interested only in free-space propagation, the computation of the far-field limit would be of academic interest. However, if the propagation medium is structured, the split-step method can accommodate the effects of the structure without further approximation.

### 3.0.3 Fresnel Diffraction

Fresnel diffraction is best illustrated by the development of a focus as a field propagates from the plane of the aperture stop. Goodman presents examples of Fresnel diffraction from the aperture stop itself (Section 4.5), but this is intrinsically part of the much more demanding calculation of the nonuniform field entering the aperture stop. The ray-optics example used computed optical paths to the focal plane to estimate this field. For our purposes here the top-hat form with an appropriate phase variation will be used. The spherical wave to aperture distance might be used as a surrogate:

$$\psi(\zeta) = \exp \left\{ ikf \left( 1 - \sqrt{1 - \zeta^2/f^2} \right) \right\} \text{ for } \zeta < D/2. \quad (38)$$

On the other hand, the Fresnel approximation shows that an aperture distribution with quadratic phase, namely

$$\psi(\zeta) = \exp \left\{ ik\zeta^2 / (2f) \right\} \text{ for } \zeta < D/2, \quad (39)$$

is consistent with the Fourier-transform relation between the uniform aperture and the focal-plane PSF. The aperture fields (38) and (39) are nearly equal for large  $f/D$  ratios.

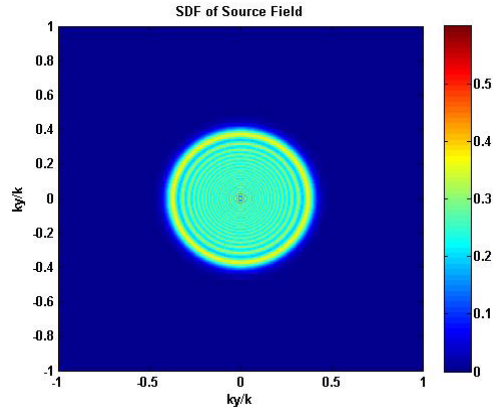


Figure 5: Spectral density function plotted against normalized spatial wavenumber for quadratic-phase starting field.

Sampling requirements are driven by the extreme phase variation at optical frequencies ( $k > 10^5$ ). This is not surprising that near-wavelength sampling is necessary considering that the distribution of Huygens-Fresnel sources are close to the initiation. A near-wavelength source sampling is also necessary for the Huygens-Fresnel construction; however, the computation can be confined to the small support of the point spread function. Trial and error showed that sampled fields similar to the Fraunhofer example could be used only for wavelengths in the millimeter range. The focal length and aperture size were adjusted to provide a large aperture in wavelengths. The possibility of moving the reference plane closer to the focal plane was not explored.

To demonstrate the sampling requirements, Figure 5 shows focal-plane spectral density plotted against wavenumber normalized by  $k$ . An aperture diameter of 60 mm was used with  $k = 10$  reciprocal millimeters ( $f = 477.5$  GHz). The quadratic source field defined by (39) with  $f = 140$  mm was used. The significant portion of the spectral intensity occupies nearly 50% of the range of non-evanescent waves, which is well beyond the narrow-angle scatter limits.

Even so, the field in any forward plane can be computed by applying the Fourier-domain propagator. Figure ?? shows a vertical-plane cut of the field intensity computed at 111 planes centered on the nominal focal distance and separated by 1 mm. The  $x$  distance is measured from the exit plane, which accounts for the displacement from 140 mm. Figure 6 shows the detail of the Focal plane intensity. It is imperceptibly different from the scaled Fourier transform of the Fourier-transform of the aperture stop as predicted by (30).

The assistance of Dennis Hancock in clarifying concepts and optical methodology is gratefully acknowledged. <http://dennishancock.com/>

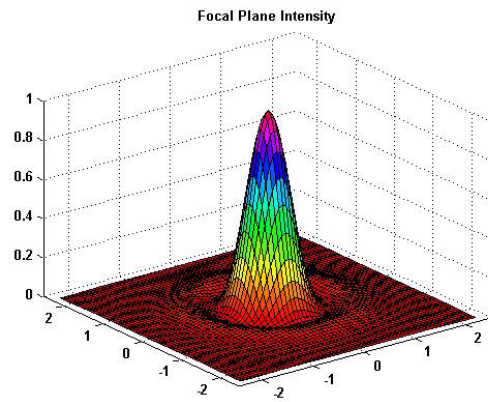
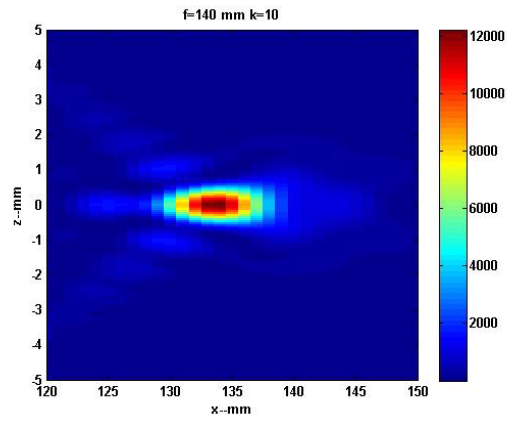


Figure 6: Focal plane field intensity.

## References

- [1] Charles L. Rino. *The Theory of Scintillation with Applications in Remote Sensing*. John Wiley and Sons, Inc., New York, 2011.
- [2] J. A. Kong. *Electromagnetic Wave Theory: Second Edition*. John Wiley & Sons, New York, 1986.
- [3] M. V. Berry. Focusing and twinkling: Critical exponents from catastrophes in non-Gaussian random short waves. *J. Phys. A: Math. Gen.*, 10(12):2061–2081, 1977.
- [4] Joseph W. Goodman. *Introduction to Fourier Optics*. Roberts and Company, Connecticut, 2005.
- [5] M. Born and E. Wolf. *Principles of Optics*. Cambridge University Press, 1999.
- [6] Mireille Levy. *Parabolic Equation Methods for Electromagnetic Wave Propagation*. Institute of Electrical Engineers, United Kingdom, 2000.
- [7] N. Delen and B. Hooker. Verification ofn comparison of a fast fourier transform-based full diffraction method for tilted and offset planes. *Applied Optics*, 40(21):3525–3531, 2001.
- [8] Hoc D. Ngo and Charles L. Rino. Wave scattering functions and their application to multiple scattering problems. *Waves in Random Media*, 3(3):199–210, 1993.